CHARACTERIZATION OF LASER SCANNERS FOR DETECTING CRACKS FOR POST-EARTHQUAKE DAMAGE INSPECTION

*Engin Burak Anil[1], Burcu Akinci[1], James H. Garrett[1], Ozgur Kurc[2]

[1]*Carnegie Mellon University*
Department of Civil and Environmental Engineering
5000 Forbes Ave., Pittsburgh, PA, 15213
*(*Corresponding author: eanil@andrew.cmu.edu)*

[2]*Middle East Technical University*
Department of Civil Engineering
Ankara, Turkey, 06800

ABSTRACT

Objective, accurate, and fast assessment of damage to buildings after an earthquake is crucial for timely remediation of material losses and safety of occupants of buildings. Laser scanners are promising sensors for collecting geometrical data regarding the damaged states of buildings, as they are able to provide high coverage and accuracy at long ranges. Yet, we have limited knowledge on the performance of laser scanners for detecting earthquake damage, and requirements of such data collection. This paper focuses on characterizing the performance of laser scanners for detecting thin cracks for damage assessment of reinforced concrete frames. We identified a series of crack parameters based on the state-of-the-art damage assessment codes and standards. Similarly, we identified parameters, which affect the performance of laser scanners for detecting cracks, based on prior research in this area. We studied the width, depth, and orientation of cracks; sampling interval of the scanner, and the range of the laser beam from the surface. Effects of these parameters on the detection of the minimum crack size were determined in an experimental setting. An automated algorithm was used to analyze the data. The results show that it is possible to detect as small as ~1mm cracks.

KEYWORDS

Earthquake; Damage assessment; Laser scanning; Crack detection; Reinforced concrete frames

INTRODUCTION

Earthquake damaged buildings must be inspected to determine the nature and severity of damage, to assess the safety of the structure, and to design strengthening measures. Currently accepted practices of damage assessment rely on visual observation of damage and manual interpretation of reports and sketches prepared by the inspectors in the field (FEMA, 1999a, 1999b). Inspection requires experience and knowledge about structural behavior. Typically, earthquake damage is inspected by structural engineers and trained building inspectors.

Visual observation, manual reporting and interpretation have been shown to have some drawbacks. First, important details can be missed, misinterpreted, or field measurements and calculations can be incorrect during the inspection. Second, visual inspections and reports may not be as thorough as required (Kempton et al., 2001; Menches et al., 2008; Phares et al., 2001). Finally, interpretation of the reports and overall results of the inspection can vary (Kempton et al., 2001; Menches et al., 2008; Phares et al., 2001).

Laser scanning technology has been shown to be effective for identifying damage indicators, such as cracks, displacements, deflected shapes, and surface defects (Olsen et al. 2009; Park et al. 2007). Laser scanners have several advantages, such as high resolution, high range, high coverage (i.e., being able to image entire surfaces as opposed to taking points measurements), and independence of light (Park et al., 2007). On the other hand, laser scanners have limitations and unique challenges for imaging thin and sharp features, such as cracks (Tang et al., 2009; Tuley et al., 2005). As with any measurement equipment, measurements contain noise and errors. Additionally, the phenomenon called mixed pixels can result in incorrect measurements (Tang et al., 2009). However, from a damage detection perspective, we have limited knowledge on the performance of laser scanners for detecting cracks.

The research described in this paper incorporates a detailed experimental program for identifying limits of laser scanners for imaging cracks, specifically for the purpose of damage assessment of reinforced concrete buildings. Three specific goals were pursued: 1) crack parameters were identified based on damage assessment guidelines and accepted practices of structural engineering; 2) laser scanning parameters were identified based on previous research; 3) experiments were performed on artificially created blocks to test the interaction of the crack parameters and laser scanner parameters (Figure 1).

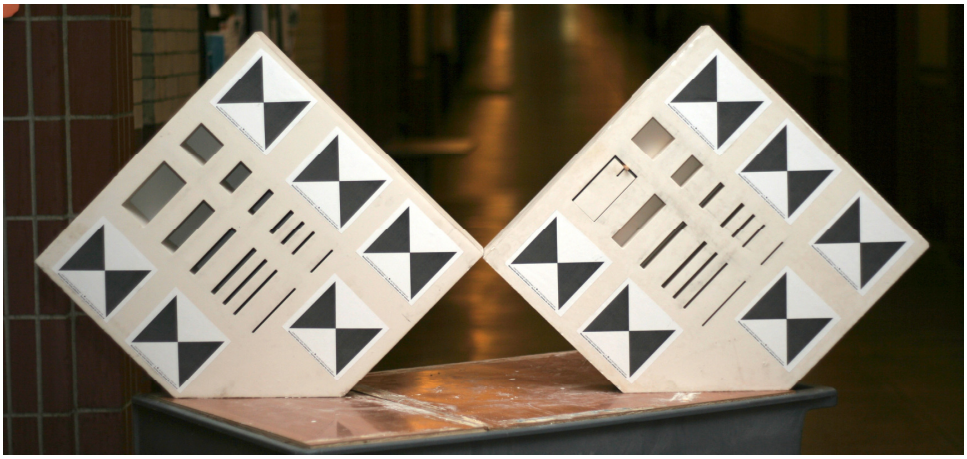

Figure 1 - The blocks have 10 cm (left block) and 5 cm (right block) depth and various crack sizes. The 5 cm block has a moveable piece that allows adjustment of the crack size. The blocks are shown in 45º orientation. Six targets were placed on each block. These targets were used to establish a reference coordinate system to be used by the algorithm for crack measurement

Specifically, the range and resolution of the scanner, and width, depth, and orientation of cracks were tested to identify the effects of these parameters on the detection of cracks. Laser beam size was tested implicitly as it is a function of the range. A reference configuration was selected and only one parameter was varied in each set of experiments. Every configuration was scanned 5 times with two different scanners (i.e., a PTOF scanner and an AMCW scanner). The data was analyzed using a voting method (Tang et al., 2009). The result is a set of graphs, which show the minimum crack size a laser scanner can capture given the scan parameters.

THE TEST-BED

The test-bed consists of two hydro-stone blocks with 5 cm and 10 cm depths and two laser scanners, which represent the two widely used scanning technologies (Figure 1). The first scanner is a pulsed time-of-flight (PTOF) scanner (Leica, 2007). The second one is an amplitude modulated waveform (AMCW) scanner (Zoller+Fröhlich, 2005). Crack width, crack orientation, crack depth were identified as damage assessment related parameters for cracks (FEMA, 1999a). Hence, the hydro-stone blocks were prepared to have different crack widths, orientation, and depths.

There is no generic list of crack sizes that applies to every type of structural behavior (FEMA, 1999a). Therefore, we used an inclusive list of crack sizes that are used for all of the behavior modes defined in the FEMA guideline (Table 1). The 5cm block has a moveable piece that was used to set the crack width to 1.25 mm. Due to the limitations of the production process, the actual crack widths are different than the planned crack widths (Table 1).

Table 1 - Crack parameters used in the experiments. Due to the limitations of the water-jet in adjusting the width of the cracks, the actual crack widths are larger than the planned widths.

Parameter	**Value**
Planned crack widths	0.8, 1.6, 3.2, 4.8, 6.4, 9.5, 25, 50 mm
Actual crack widths	1.25, 3.5, 4.6, 6.4, 10.8, 27, 52.5 mm
Crack orientations	0º, 45º, 90º
Crack depths	5, 10cm

Orientation of the cracks depicts the behavior of the component (e.g., shear, flexure) (FEMA,1999a). Additionally, sampled imaging devices have an anisotropic character (Reichenbach et al., 1991). Therefore, alignment of the feature and the sampling grid have an impact on the detection (Lichti and Jamtsho, 2006; Reichenbach et al., 1991). Additionally, elliptic beam footprint, which is a result of the faster vertical motion of scanners impacts the mixed pixel behavior (Tang et al., 2009). We tested three different crack orientations (i.e., 0º, 45º, and 90º) by placing the blocks on its sides (Figure 1).

Crack depth is expected to interact with the mixed pixel behavior of the laser scanners (Hebert and Krotkov, 1991; Tang et al., 2009). We used 5 cm and 10 cm as the crack depths. The 5 cm crack depth roughly corresponds to the case where the crack penetrates through the concrete cover and reaches the concrete core for a regular component. The 10 cm depth was chosen to be able to observe the behavior of scanners at larger depths.

The main parameters that control the resolution of laser scanners are sampling interval, which is the distance between laser beams, and beam width (Lichti & Jamtsho, 2006). The effects of beam size were implicitly considered through range and angle of incidence. In order to satisfy the Nyquist frequency

sampling requirements for the 1.25 mm crack, we selected 0.5 mm as the smallest sampling interval (Table 2) (Lichti & Jamtsho, 2006). We also considered a sampling interval of 86% of the laser beam width, which corresponds to the theoretically optimal angular resolution for laser scanners as discussed in Lichti and Jamtsho (2006). The waveform scanner is limited to three preset sampling interval values (Table 2). Additional configurations were used with the time of flight scanner to match those of the waveform scanner for comparison. Finally, intermediate values were tested with the time of flight scanner. Four ranges were considered in the experiments. As the lowest range, 10 m was used. We tested up to 40 meters by 10 meter increments. We considered 0º, 30º and 60º incidence angles.

Table 2 - Sampling intervals used for the two scanners at 10 m range. The reference sampling was selected as 0.5 mm for the PTOF scanner and 0.0018º for the AMCW scanner

Scanner	**Sampling intervals (mm)**							
PTOF	0.5	1.5	3.1	4.3	6.3	10	12.6	15
AMCW	-	-	3.1 (0.0018º)	-	6.3 (0.0036º)	-	12.6 (0.0072º)	-

Since it is not practical to test all of the combinations of parameters, one parameter was tested at a time while fixing the other parameters at a reference configuration. For example, the range was varied, while the resolution and orientation were fixed. The reference configuration was set as 0.5 mm and 3.1 mm sampling intervals for the PTOF scanner and the AMCW scanner respectively; 10 m range; and vertical crack orientation. At all times, the incidence angle was fixed at 0º in the reference configuration.

Point Classification Algorithm

In order to analyze the data consistently across scans (i.e., classifying the points using the same metrics), we used an automated method, which can classify points as being a crack point or a surface point. The method is based on the voting method presented in Tang et al. (2009). A slice is extracted from the scan data across each block. Classification is performed in local neighborhoods of fixed size (i.e., number of points). The size of the local neighborhoods was selected to maximize the detection of cracks and minimize false positives for dense scans as well as sparser scans. We used 80% of the point density in each scan as the neighborhood size. For example, if the point density is 100 points/cm^2, the neighborhood size is 80 points.

For every window (i.e., local neighborhood), the standard deviations of the distance of points within the window from the block surface are computed. A threshold is used to classify the points as being on the block surface or inside the crack. More precisely, if the number of points that are within 2σ distance to the surface are less than the number of points that are farther than 2σ within a window, then the window position is marked as a crack. The range standard deviation (σ) is computed for every scan on an undamaged section of the block with the assumption that noise is uniform over the surface of the block. Every point on the slice was tagged either as belonging to the surface or a crack.

RESULTS

The results of the analyses are presented and discussed in this section. The graphs present the minimum crack widths that are detected using the sliding window algorithm using different scanner configurations and crack parameters. Every data point in the graphs means that all of the cracks that are equal to or greater than that value are detected.

The Effect Of Sampling Interval On Minimum Detected Crack Size

Using the PTOF scanner, the smallest crack (1.25 mm) is detected using 0.5 mm and 1.5 mm sampling intervals at 10 meters. The 1.25 mm crack is missed using the 86% of the beam width as the sampling interval. As the sampling interval increases the smallest detected crack width increases. With the PTOF scanner, at sampling intervals larger than 6 mm, the smallest crack widths detected are different for 5 cm and 10 cm deep cracks. As the sampling interval increases, the differences between the smallest detected crack on the 5 cm deep block and the 10 cm deep block increase.

Using the AMCW scanner's highest resolution (3.4 mm at 10 m range) it is possible to detect the smallest crack width of 1.25 mm (Figure 2). Using the same sampling interval, the 1.25 mm crack cannot be detected with the PTOF scanner. The difference in the results of the two scanners can potentially be explained by the scanners' mixed-pixel behaviors. The PTOF scanner records the foreground distance if a proportion of the laser falls on the surface (Tang et al. 2009). Since, the laser spot is much larger than the crack width (~5 mm > 1.25 mm), the surface distance is recorded. On the other hand, the distance recorded by the AMCW scanner can be anywhere between the two surfaces depending on the foreground and the background distances. Similar difference in behavior of the two scanners is observed at 6.4 mm sampling interval (Figure 3).

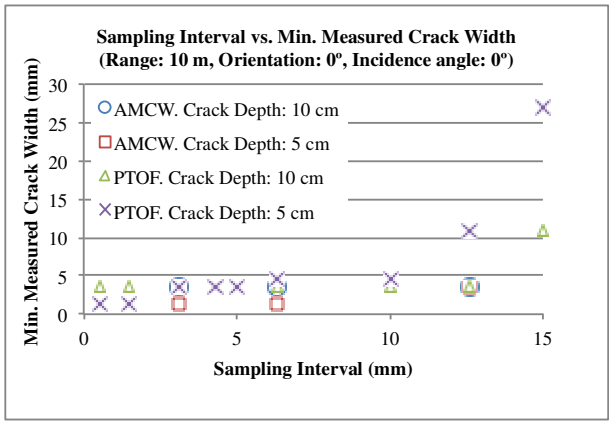

Figure 2 The smallest crack widths that were detected for different sampling intervals. 1.25 mm crack is detected using a sampling interval denser than 1.5 mm for the PTOF scanner or 6.3 mm for the AMCW scanner

Effect of Range on Minimum Detected Crack Size

The second set of results present the relationship between the minimum crack widths that are detected by the algorithm for different range values (Figure 3a and b). The angle of incidence, and crack orientation are fixed at reference values. Sampling intervals for the AMCW scanner can only be set to angular values, which results in different sampling intervals in millimeters at different ranges. Therefore, two scanners were evaluated separately. A fixed sampling interval of 0.5 millimeters at all ranges is used with the PTOF scanner (Figure 3a). The AMCW scanner was set to 0.018º sampling interval which produces 3.1, 6.3, 9.4, and 12.6 millimeters sampling intervals at 10, 20, 30, and 40 meters respectively (Figure 3b).

Using the PTOF scanner, 1.25 mm crack can be detected at any range upto 40 m, which is the longest range we tested. Using the AMCW scanner, 1.25 mm crack can be detected upto 20 m. At longer ranges, the performance degrades gradually. The different performance of the two scanners in terms of range can be explained by comparing their range noises (i.e., standard deviation of range). We measured the range noise of the PTOF scanner to be between 1.43-1.54 millimeters at 10m - 40 m range on the tested surface. On the other hand, the AMCW scanner has a range noise between 2.72-9.53 millimeters and shows an

increasing trend with range. High spread of points prohibits the algorithm to correctly classify points correctly.

Effect of Crack Orientation on Minimum Detected Crack Size

The third set of results presents the minimum crack width detected for varying crack orientations (Figure 4). Specifically, vertical, 45° diagonal, and horizontal cracks are scanned. The sampling interval are different for the two scanners. The AMCW scanner is set to 3.1 mm. The PTOF scanner is set to 0.5 mm and also to 3.1 mm for comparison with the AMCW scanner.

The results show that using the AMCW scanner the 1.25 mm crack can be detected at any orientation with 3.1 mm sampling interval. Using the same sampling interval and the PTOF scanner, the 1.25 mm crack is only detected when then crack is horizontal, and at 45° and 90° the smallest crack that is detected is 3.5 mm wide. Using 0.5 mm sampling interval, 1.25 mm crack can be detected at 0° and 90° orientation with the PTOF scanner. The PTOF scanner is not able to detect the 1.25 mm crack at 45° crack orientation using any of the scanner configurations tested in this study.

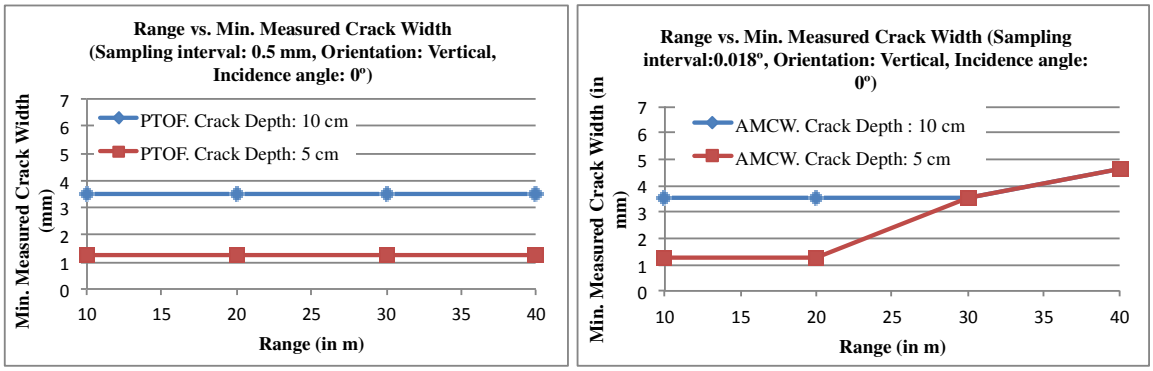

(a) (b)

Figure 3 – The smallest crack widths detected at different ranges and using a fixed sampling interval. The sampling interval is fixed in linear units for the PTOF scanner (a). The AMCW scanner is set to 0.0018° angular sampling interval, which produces different intervals in linear units at different ranges

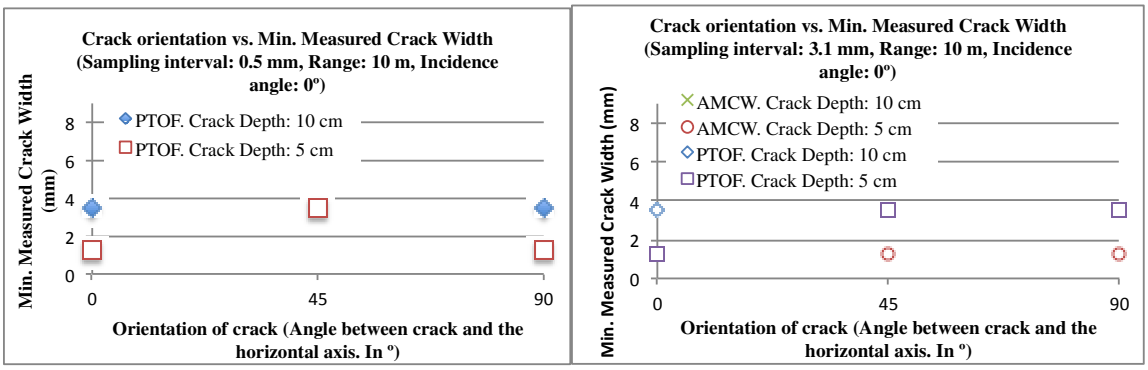

(a) (b)

Figure 4 – Minimum crack widths detected at different crack orientations. Range is fixed to 10m. Sampling interval of the PTOF scanner is set t0 0.5 mm and 3.1 mm. The AMCW scanner is set to 3.1 mm at 10 m range.

CONCLUSIONS

The results show that all of the crack widths we tested in this study can be identified using laser scanners if the scanning parameters are set favorably. We observed that range is a limiting factor on the performance of the AMCW scanner. Beyond 20 m range, the performance of the AMCW scanner gradually degrades. For the PTOF scanner, the range is not a limiting factor. The smallest crack width tested in this study (1.25 mm) cannot be detected using the PTOF scanner if the crack is aligned diagonally. For the PTOF scanner, 1.5 mm is the largest sampling interval that should be used if millimeter wide cracks are scanned. For the AMCW scanner, the sampling interval can be as large as 6.3 mm.

The results of this study can be used in several ways. Using the graphs in this study, engineers in the field can assess whether certain cracks will be detectable in scans given the properties of cracks, scanner technology and scanner parameters. The graphs can also be used to determine appropriate scanner parameters for detecting cracks of a certain size and orientation. Finally, the crack widths and orientations used in this study can be related back to damage severities in damage assessment guidelines (e.g., moderate, significant, etc.) and the results of this study can be used to assess what damage severities can be identified using a certain scan data.

The results point to several potential research directions. First, there are certain differences between the artificial cracks on the hydro-stone blocks and real cracks. For example, the edges and shapes of real cracks are not as smooth and straight as those on the hydro-stone blocks. Therefore, we are working on collecting data on real cases and comparing the results presented in this paper to those obtained from real cases. Second, for damage assessment we are more interested the width of cracks. We are working on assessing the accuracy of the width measurements using the collected data.

REFERENCES

FEMA. (1999a). FEMA 306 - Evaluation of Earthquake Damaged Concrete and Masonry Wall Buildings: Basic Procedures Manual. Washington, D.C.: FEMA.

FEMA. (1999b). FEMA 307 - Evaluation Of Earthquake Damaged Concrete And Masonry Wall Buildings, Technical Resources. Washington, D.C.: FEMA.

Hebert, M., & Krotkov, E. (1991). 3D Measurements From Imaging Laser Radars: How Good They Are? *International Workshop on Intelligent Robots and Systems IROS '91*. Osaka, Japan.

Kempton, J., Nichol, S., Anumba, C., & Dickens, J. (2001). Surveyor Variability In Large-Scale House Condition Surveys. *Structural Survey*, *19*(4), 156–162. doi:10.1108/02630800110406658

Leica. (2007). *ScanStation 2 Data Sheet*. Retrieved from http://hds.leica-geosystems.com/en/Leica-ScanStation-2_62189.htm

Lichti, D. D., & Jamtsho, S. (2006). Angular Resolution Of Terrestrial Laser Scanners. *Photogrammetric Record*, *21*(114), 141–160.

Menches, C. L., Markman, A. B., & Jones, R. J. (2008). Innovative Method for Investigating the Facility Damage Assessment Process. *Architectural Engineering Conference (AEI) 2008*. Denver, Colorado.

Olsen, M. J., Kuester, F., Chang, B. J., & Hutchinson, T. C. (2009). Terrestrial Laser Scanning-Based Structural Damage Assessment. *Journal of Computing in Civil Engineering*, *24*(3), 264 – 72.

Park, H. S., Lee, H. M., Adeli, H., & Lee, I. (2007). A New Approach For Health Monitoring Of Structures: Terrestrial Laser Scanning. *Computer aided civil and infrastructure engineering*, *22*, 19–30.

Phares, B. M., Rolander, D. D., Graybeal, B. A., & Washer, G. (2001). Reliability Of Visual Bridge Inspections. *Public Roads*, *64*(5).

Reichenbach, S. E., Park, S. K., & Narayanswamy, R. (1991). Characterizing Digital Image Acquisition Devices. *Optical Engineering*, *30*(2), 170–177.

Tang, P., Akinci, B., & Huber, D. (2009). Quantification Of Edge Loss Of Laser Scanned Data At Spatial Discontinuities. *Automation in Construction*, *18*(8), 1070–1083.

Tuley, J., Vandapel, N., & Hebert, M. (2005). Analysis and Removal of Artifacts in 3-D LADAR Data. *Proceedings of the IEEE International conference on Robotics and Automation* (pp. 2203–2210).

Zoller+Fröhlich. (2005). *Z+F Imager5003 Technical Specification*. Zoller+Frohlich, Inc.